

Low-Density Structures in the Local Universe.

II. Nearby Cosmic Voids

A. Elyiv^{1,2}, I. Karachentsev³, V. Karachentseva¹, O. Melnyk^{2,4}, D. Makarov³

¹ *Main Astronomical Observatory, National Academy of Sciences, Kiev, 03680 Ukraine*

² *Institut d'Astrophysique et de Geophysique, Université de Liège, Liège, B5C B4000 Belgium*

³ *Special Astrophysical Observatory of the Russian AS, Nizhnij Arkhyz 369167, Russia*

⁴ *Astronomical Observatory, Taras Shevchenko National University of Kiev, 04053 Ukraine*

Abstract

We present the results of the search for spherical volumes containing no galaxies with luminosities brighter than the Magellanic Clouds in the Local Supercluster and its vicinity. Within a distance of 40 Mpc from us, 89 cosmic voids were discovered with the diameters of 24 to 12 Mpc, containing no galaxies with absolute magnitudes brighter than $M_K < -18.4$. A list of these voids and the sky distribution maps are given. It was found that 93% of spherical voids overlap, forming three more extended percolated voids (hypervoids). The largest of them, HV1, has 56 initial spherical cells and extends in a horseshoe shape, enveloping the Local Volume and the Virgo cluster. The Local Void (Tully, 1988) in the Hercules–Aquila region is the closest part of the HV1. Another hypervoid, HV2, contains 22 spherical voids in the Eridanus constellation, and the third compact hypervoid (HV3) comprises 6 spherical cells in the Bootes. The total volume of these voids incorporates about 30% of the Local Universe. Among 2906 dwarf galaxies excluded from the original sample ($n = 10502$) in the search for spherical volumes, only 68 are located in the voids we have discovered. They are characterized by late morphological types (85% are Ir, Im, BCD, Sm), absolute magnitudes M_B ranging from -13.0 to -16.7 , moderate star formation rates ($\log \text{SSFR} \sim -10 M_\odot \text{yr}^{-1} L_\odot^{-1}$) and gas reserves per luminosity unit twice to three times larger than in the other dwarf galaxies located in normal environments. The dwarf population of the voids shows a certain tendency to sit shallow near the surfaces of cosmic voids.

Keywords: cosmology: large-scale structure of Universe.

1 INTRODUCTION

The main element in the picture of the large-scale structure of the Universe, often referred to as the “Cosmic Web”, are the vast low-density regions, separated by the “walls” and filaments. The first observational evidence for the existence of giant cavities (voids) appeared about 30 years ago [1, 2, 3], but the concept of cosmic voids was implemented in common practice with the advent of mass surveys of galaxy redshifts. According to the current estimates, the sizes of voids span a wide range of extents from the supervoids with the diameters of about 200 Mpc [4] to mini-voids covering about 3–5 Mpc [5]. There is a conception that the typical number density of galaxies in cosmic voids is at least an order of magnitude lower than global mean density.

A lot of studies can be found in the literature, examining the statistics of sizes and shapes of voids, as well as the features of their population. A recent review of these studies was presented by van de Weygaert and Platen [6]. Different authors have used various algorithms for identifying the voids in mass sky surveys. Some of them suggest a complete absence of galaxies in the voids up to a fixed luminosity level. Other criteria allow the possibility of presence of a small number of galaxies with normal luminosity in the low-density regions. In the latter case, these regions should rather be called lacunas instead of voids.

Two important questions still remain unresolved: 1) whether there are volumes of space, completely devoid of galaxies, 2) if there are any signs of the void expansion in the kinematics of galaxies surrounding it. The answers to these questions are closely related to the choice of the most plausible scenario of the formation of the large-scale structure of the Universe [7, 6]. It is evident that the best opportunity to explore the dwarf population of the voids and the kinematics of galaxies around them is provided by the nearest voids. Compiling the atlas of nearby galaxies, Tully and Fisher [8] have discovered a giant empty region in the Aquila–Hercules constellations, which starts immediately at the threshold of our Local Group of galaxies, and occupies about a quarter of the entire sky. Inside this Local Void only two dwarf galaxies were found to date: KK 246 [9] and ALFAZOA J1952+1428 [10] with absolute B -magnitudes of -13.7^m and -13.5^m , respectively. The analysis of the data on the radial velocities and distances of the galaxies in the vicinity of the Local Void points to an expansion of its frontiers at a velocity of about 300 km/s [11].

Using the 2dFGRS [12] and SDSS¹ [13] galaxy redshift surveys, Patiri et al. [14] and Hoyle et al. [15] have identified a large number of distant voids at the characteristic distances of $z \sim 0.1$. However, we have not found in the literature any systematic lists of voids in a closer volume on the scale of $z \sim 0.01$. An enumeration of nearby voids in the southern and northern sky, indicating their rough outlines can be found in the Fairall’s manuscript [16]. Pustilnik and Tepliakova [17] have investigated the properties of dwarf galaxies in the region of the Lynx–Cancer void. Saintonge et al. [18] noted the presence of a nearby ($V \sim 2000$ km/s) void in the Pisces constellation according to the ALFALFA survey data [19].

In the first paper of this series [20], applying the percolation method we have identified the diffuse agglomerates of galaxies in the Local Supercluster, which are located in the regions of low matter density, and discussed the properties of the most populated non-virialized structures. In this paper we describe the algorithm for identifying the voids in the Local Supercluster, give a list of nearby (within 40 Mpc) voids and briefly discuss the properties of dwarf galaxies located in the nearby voids.

2 ORIGINAL SAMPLE OF GALAXIES

To search for voids in the Local Universe we used a sample of 10 502 galaxies with radial velocities $0 < V_{LG} < 3500$ km/s relative to the centroid of the Local Group. The sample includes both the northern and southern sky, except for the low galactic latitudes $|b| < 15^\circ$. For these galaxies, presented in recent versions of the HyperLeda² [21] and NED³ databases we have refined their angular dimensions and morphological types. Since the

¹Sloan Digital Sky Survey (<http://www.sdss.org>).

²Lyon Database for Physics of Galaxies
(<http://leda.univ-lyon1.fr>).

³NASA/IPAC Extragalactic Database
(<http://nedwww.ipac.caltech.edu>).

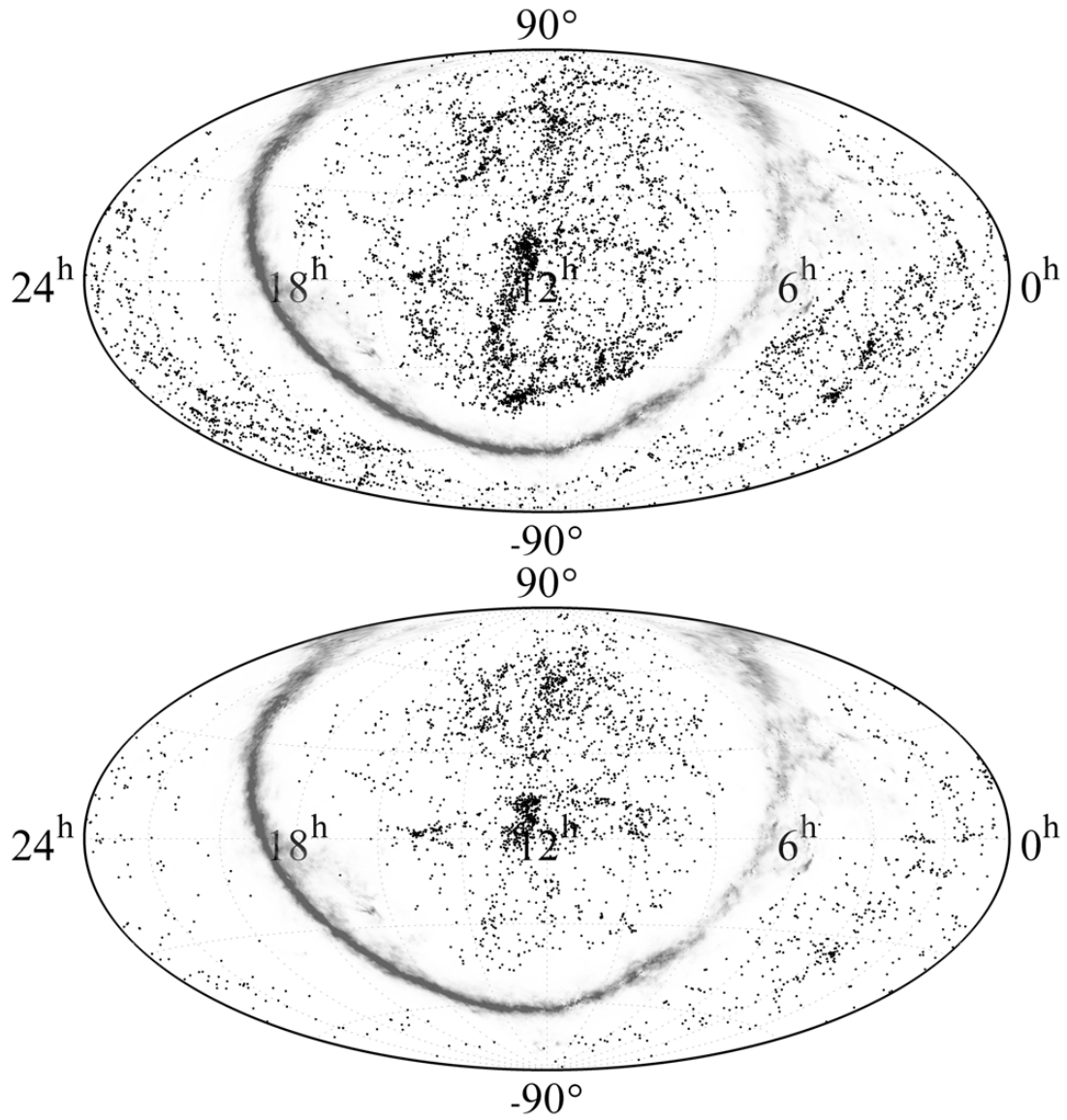


Figure 1: The distribution of 7596 bright (top panel) and 2096 dwarf (bottom panel) galaxies with $V_{LG} = 0\text{--}3500$ km/s in equatorial coordinates. The region of significant Galactic absorption with $A_B > 2.0^m$ is described by a ragged gray stripe.

stellar mass of the galaxy is best expressed through its K -band luminosity, we have used the K_s -luminosities of galaxies from the 2MASS survey [22]. In the absence of these data, we determined the apparent K -magnitudes from the apparent B -magnitudes and average color index $\langle B - K \rangle$ separately for each morphological type according to [22]. From the original sample, we have excluded faint galaxies with $K > 15.0^m$, and objects with negative radial velocities. At the Hubble parameter of $H_0 = 73$ km/s/Mpc the distance modulus for the far boundary of our sample corresponds to $m - M = 33.4^m$. In order to have the same conditions for the void identification both in the near and far regions of our volume, we have excluded from the analysis the dwarf galaxies with absolute magnitudes fainter than $M_K = -18.4$. This threshold is roughly equivalent to the luminosity of the Small Magellanic Cloud-type dwarfs. At that, the distances to the galaxies were determined by their radial velocity with the H_0 given above.

The top and bottom panels of Fig. 1 show the sky distribution of 7596 bright galaxies with $M_K < -18.4$ and 2906 dwarf galaxies, excluded from the void identification procedure, respectively. Both sub-samples show the effects of clustering into groups and clusters, as well as the concentration to the equator of the Local Supercluster. The distribution of dwarfs is affected by their over-clustering in the volumes of the nearby Virgo cluster and the Canes Venatici I cloud, as well as high density of galaxies with known redshifts in the SDSS survey [13] region.

3 VOID IDENTIFICATION ALGORITHM

For each of the 7596 galaxies with $M_K < -18.4$ within $D = V_{LG}/73 = 48$ Mpc the Cartesian equatorial coordinates X, Y, Z were calculated. Then, in this volume, applying the galactic latitude restriction, we searched for the maximum radius R for a sphere which does not contain any galaxies. For this purpose, we have carried out a search of all possible coordinates of the circumcenter and the radius of the sphere. The search increment has been set at 1.5 Mpc for the elapsed time reasoning (a compromise between the accuracy and required computer time). The limiting conditions were set so that the center of the sought void would lie within $D = 48$ Mpc and not be located in the cone of the Milky Way $|b| < 15^\circ$.

Further, we looked for the following void with the maximum radius and containing no galaxies. The limiting conditions were supplemented with a new constraint: the center of the desired void has to be located outside the volume, occupied by the previous void. This procedure was repeatedly iterated accounting for the locations and sizes of all previous voids. This process was in progress until the number of voids has reached $n \geq 100$. The result is a collection of 179 empty spherical volumes with the radii of 12 to 6 Mpc, quite a few of which partially overlap each other.

The applied algorithm does obviously include several parameters, the choice of which affects the final list of voids. One of them is the minimum distance of the void center to the boundaries of the volume, as well as the minimum distance between the centers of the voids. Another parameter is the threshold absolute magnitude of the dwarf galaxies ($M_K = -18.4$), the possible presence of which in the empty volume is ignored. The third parameter is the minimum radius of the spherical void ($R_{\min} = 6.0$ Mpc), which terminates the application of the algorithm.

Attempting to reject the sphericity of the identified empty volumes, as did Tikhonov and Karachentsev [5] significantly complicates the algorithm. In addition, a comparison of the SDSS DR7 data with the galaxy distribution of the Millennium 1 model catalog by Tavasoli et al. [23] has shown that the shape of voids tends to be spherical. If needed,

Table 1: The list of spherical voids in the Local Universe

No.	D , Mpc	RA, deg	Dec, deg	R , Mpc	r , deg	Note	No.	D , Mpc	RA, deg	Dec, deg	R , Mpc	r , deg	Note
(1)	(2)	(3)	(4)	(5)	(6)	(7)	(1)	(2)	(3)	(4)	(5)	(6)	(7)
38	8.7	301	0	7.5	59	HV1, Aqr	47	30.9	8	47	7.5	14	HV1
9	16.1	288	-28	9.0	34	HV1, Sgr	122	31.2	279	29	6.0	11	HV1
116	16.6	85	-5	6.0	21	HV1, Ori	26	31.5	141	-72	7.5	14	HV2
34	17.6	275	20	7.5	25	HV1, Her	161	31.8	16	-28	6.0	11	HV2
27	18.4	117	24	7.5	24	HV1, Gem-Leo	117	31.9	278	-45	6.0	11	HV1
136	19.1	360	45	6.0	18	HV1, And	159	32.0	329	-8	6.0	11	HV1
147	20.1	347	4	6.0	17	Psc-Peg	100	32.1	258	25	6.0	11	HV1
144	21.0	18	25	6.0	17	HV1, Psc	114	32.3	83	68	6.0	11	HV1
90	21.5	238	-25	6.0	16	HV1, Sco-Lib	35	32.4	79	-76	7.5	13	HV2
119	21.5	283	50	6.0	16	HV1, Dra	146	32.4	347	-52	6.0	11	HV2
135	21.8	309	12	6.0	16	HV1, Del	148	32.7	35	43	6.0	11	HV1
31	23.9	248	-70	7.5	18	HV1, Aps	157	32.8	32	-30	6.0	11	HV2
120	25.3	68	-71	6.0	14	HV2	156	32.9	29	33	6.0	11	HV1
107	25.6	265	50	6.0	14	HV1	2	33.1	339	39	12.0	21	HV1
118	25.6	279	-45	6.0	14	HV1	49	33.3	319	27	7.5	13	HV2
130	26.0	299	-44	6.0	13	HV1	165	33.5	22	-16	6.0	10	HV2
39	26.1	80	7	7.5	17	HV1	56	33.7	3	-21	7.5	13	HV1
123	26.6	288	58	6.0	13	HV1	124	34.0	291	-68	6.0	10	HV1
42	27.0	60	26	7.5	16	HV1	166	34.3	337	-3	6.0	10	HV1
140	27.1	29	46	6.0	13	HV1	51	34.6	3	-34	7.5	13	HV2
111	27.6	90	-45	6.0	13	HV2	13	34.7	50	18	9.0	15	HV1
96	27.7	249	22	6.0	13	HV1	40	34.7	77	12	7.5	13	HV1
154	27.7	22	29	6.0	12	HV1	3	34.7	59	-60	10.5	18	HV2
143	28.0	14	-49	6.0	12	HV2	104	34.8	263	0	6.0	10	HV1
150	28.0	319	-9	6.0	12	HV1	112	35.0	90	-47	6.0	10	HV2
99	29.0	254	-15	6.0	12	HV1	44	35.4	65	10	7.5	12	HV1
151	29.1	23	-38	6.0	12	HV2	75	35.4	205	10	6.0	10	HV3
86	29.5	125	-9	6.0	12		85	35.5	239	-10	6.0	10	HV1
79	29.7	204	6	6.0	12	HV3	108	35.6	265	62	6.0	10	HV1
8	30.1	101	40	9.0	17	HV1	141	35.6	60	-22	6.0	10	HV2
95	30.5	252	11	6.0	11	HV1	72	35.7	158	0	6.0	10	

nonspherical voids can be obtained within our approach by joining two or more intersecting spherical volumes in their association: a “dumbbell”, a “boomerang” or a “string”.

4 A LIST OF EMPTY VOLUMES IN THE LOCAL UNIVERSE

The results of our search for nearby spherical voids applying the above algorithm are presented in Table 1. The table columns include: (1) the number of the void in the procedure we have adopted, when each subsequent step yields the voids of an ever smaller radius; (2) the distance to the center of the void in Mpc; (3, 4) equatorial coordinates of the void’s center in degrees; (5, 6) the linear and angular diameter of the void; (7) notes, which stipulate the location of 12 most nearby voids in the constellations, and the membership of the given empty volume in the ever more extended formations, called the hypervoids (HV).

It should be noted that the table shows only 89 voids, ranked according to the distance from the observer up to 40 Mpc, from the total number of 179.⁴ We have excluded from the list a half of the most distant voids based on the following reasoning. The distribution of the integral number of voids depending on the distance of their centers D shows that near the far border of the considered volume in the range of $D = 40\text{--}48$ Mpc, there is approximately a double excess of voids, as compared with the homogeneous distribution $n \sim D^3$. This excess is due to the decrease of the number density of galaxies with measured radial velocities in the most distant parts of the Local Universe. In addition, the lack of

⁴The whole list of 179 voids can be obtained upon request to the first author.

Table 1: (Contd.)

No.	D , Mpc	RA, deg	Dec, deg	R , Mpc	r , deg	Note
(1)	(2)	(3)	(4)	(5)	(6)	(7)
106	35.8	257	-67	6.0	10	HV1
15	35.9	324	10	9.0	15	HV1
102	35.9	106	53	6.0	10	HV1
145	35.9	303	-5	6.0	10	HV1
5	36.2	306	12	10.5	17	HV1
139	36.7	294	-10	6.0	9	HV1
4	37.2	40	-47	10.5	17	HV2
105	37.4	263	50	6.0	9	HV1
80	37.6	225	16	6.0	9	HV3
18	37.6	152	31	7.5	11	
109	37.7	117	-85	6.0	9	HV2
11	37.7	288	-23	9.0	14	HV1
12	37.9	56	31	9.0	14	HV1
91	38.0	210	71	6.0	9	
53	38.1	329	23	7.5	11	HV1
126	38.1	27	-80	6.0	9	HV2
60	38.3	2	-11	7.5	11	HV2
168	38.3	0	31	6.0	9	HV1
173	38.4	5	11	6.0	9	
97	38.6	257	33	6.0	9	HV1
160	38.7	13	-44	6.0	9	HV2
115	39.0	84	67	6.0	9	HV1
48	39.1	51	-32	7.5	11	HV2
74	39.4	216	11	6.0	9	HV3
153	39.4	18	-53	6.0	9	HV2
54	38.5	39	13	7.5	11	HV1
69	39.7	209	4	6.0	9	HV3

data on the galaxies outside the radius of 48 Mpc increases the probability of finding an empty volume and “adhesion” of these excessive voids on the far boundary.

As follows from the last column of Table 1, 83 of 89 voids overlap with each other, forming three groups of hypervoids: HV1, HV2 and HV3 with 56, 22 and 5 spherical voids, respectively. Some parameters of these hypervoids: the total volume, the minimum and maximum distance of the hypervoid surface to the observer, the distance to the centroid of the hypervoid and its position in the sky are listed in Table 2. The nearest hypervoid HV1 is actually an extended and curved bunch of empty spherical volumes, which starts just beyond the boundary of the Local Group ($D_{\min} = 1.4$ Mpc). The top panel of Fig. 2 represents the sky distribution of 56 voids, contained in HV1. The sizes of circles correspond to the angular scales of the spherical voids. Not to overshadow the other voids, the contour of the nearest void No. 38 (the front part of the Tully Local Void [8]) is described by a thick dashed line.

The HV1 hypervoid, starting from the Local Group in the Hercules–Aquila region, reaches the boundary of the considered volume and, passes round the Local Volume in a horseshoe shape, and approaches it from Gemini–Leo. The horseshoe shape of the low-density regions, covering the Virgo cluster is clearly visible in Fig. 6 of Courtois et al. [24].

Fig. 3 shows the HV1 in more detail in three projections with respect to the supergalactic plane. Since the hypervoid has a complex structure, we show it from the direction of negative and positive axes perpendicular to the considered plane, in the left and right panels of the figure, respectively. The distances to the particular plane are characterized by the scale under the figure. The upper, middle and bottom panels show the projection on the SGX–SGY, SGX–SGZ, SGY–SGZ planes, respectively. Concentric circles have an increment of 10 Mpc. We can see that HV1 departs from the supergalactic plane quite far away, up to 40 Mpc. In the SGX–SGZ and SGY–SGZ projections we can clearly see that the hypervoid envelopes the Local Group. Comparing the projections of the HV1 hypervoid in Fig. 3 with the corresponding maps of the Local and Virgo voids from Cour-

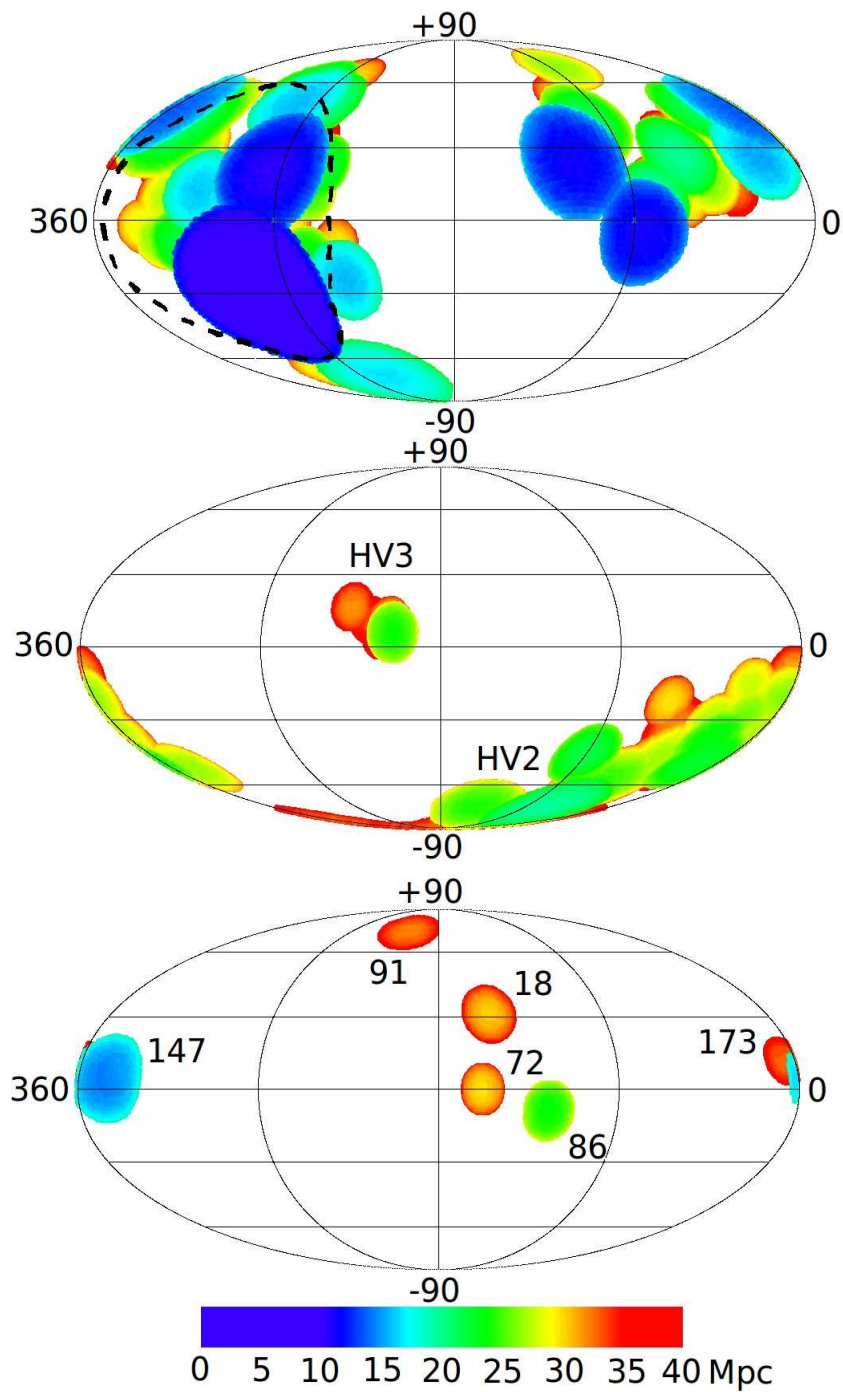


Figure 2: Distribution of voids projected on the sky in the equatorial coordinate system: the HV1 hypervoid (the top panel), the HV2 and HV3 hypervoids (the middle panel), individual voids (the bottom panel). The sizes of the circles correspond to the actual angular scales of voids. Colors show the distances to the surface of voids.

Table 2: The properties of three local hypervoids

	Hypervoids		
	HV1	HV2	HV3
Number of voids	56	22	5
Volume, Mpc ³	68469	23767	3440
D_{\min} , Mpc	1.4	19.4	23.8
D_{cen} , Mpc	13.8	30.5	35.8
D_{\max} , Mpc	46.9	47.6	45.6
RA _c , deg	22.2	2.4	14.2
Dec _c , deg	+32	−51	+10
Sky region	Pegasus	Eridanus	Bootes

tois et al. [24], we can conclude that about 2/3 of the HV1 volume coincide with the total volume of Local and Virgo voids.

The middle panel of Fig. 2 reproduces the sky distribution of 22 spherical voids, merging into the HV2 hypervoid in the region of the Eridanus and 5 voids, belonging to a more compact HV3 hypervoid in the Bootes constellation. The bottom panel of Fig. 2 presents six separate spherical voids, the surfaces of which are not in contact with other empty volumes, identified by our algorithm. It is appropriate to recall here that we have restricted ourselves to the search for voids with linear radii of at least 6 Mpc. We can assume that there are plenty of small voids that overlap with the already identified voids, thus increasing their total volume.

5 DWARF POPULATION OF NEARBY VOIDS

Summing up the volume of voids presented in Table 1, we deduce that they occupy about 30% of the considered volume of the Local Universe within 40 Mpc. This estimate takes into account the fact that the spherical voids belonging to hypervoids overlap. Searching for nearby voids we have excluded from consideration 2906 dwarf galaxies. If this population was homogeneously distributed in the volume of the Local Universe, the expected number of dwarf galaxies in the voids would amount to about 1000. Their real number, which is $N = 48$ within 40 Mpc and $N = 68$ within 48 Mpc does not reach even a tenth of expected. This means that the empty volumes, devoid of galaxies with normal luminosity remain almost empty when considering the dwarf galaxies as well.

The list of dwarf galaxies, which are located inside of 89 voids we have identified, is presented in Table 3. The columns of the table contain the following information about the galaxies: (1) the name of the galaxy, or its presence in the SDSS, 6dF, 2MASX, KUG, HIPASS, APMUKS sky surveys; (2) the equatorial coordinates for the epoch J 2000.0; (3) the line-of-sight velocity relative to the centroid of the Local Group (km/s), used to determine the distance at the parameter $H_0 = 73$ km/s/Mpc; (4) morphological type; (5) apparent B -band magnitude; (6) apparent ultraviolet magnitude m_{FUV} , ($\lambda_{\text{eff}} = 1539$ Å, FWHM = 269 Å) according to GALEX [27, 28]; (7) the flux logarithm F_{HI} in the line of neutral hydrogen (F_{HI} in the Jy×km/s units); (8) absolute magnitude; (9) the logarithm of the hydrogen mass $M_{\text{HI}} = 2.36 \times 10^5 D^2 F_{\text{HI}}$, where D is the distance in Mpc; (10) the logarithm of the star formation rate $\log \text{SFR} = 2.78 - 0.4m_{\text{FUV}}^c + 2 \log D$ in the M_{\odot}/yr units, where m_{FUV}^c is the UV value, corrected for absorption [29], and the distance D is expressed in Mpc; (11) the depth of bedding of the galaxy below the surface of the hypervoid (in Mpc); a dash in this column indicates

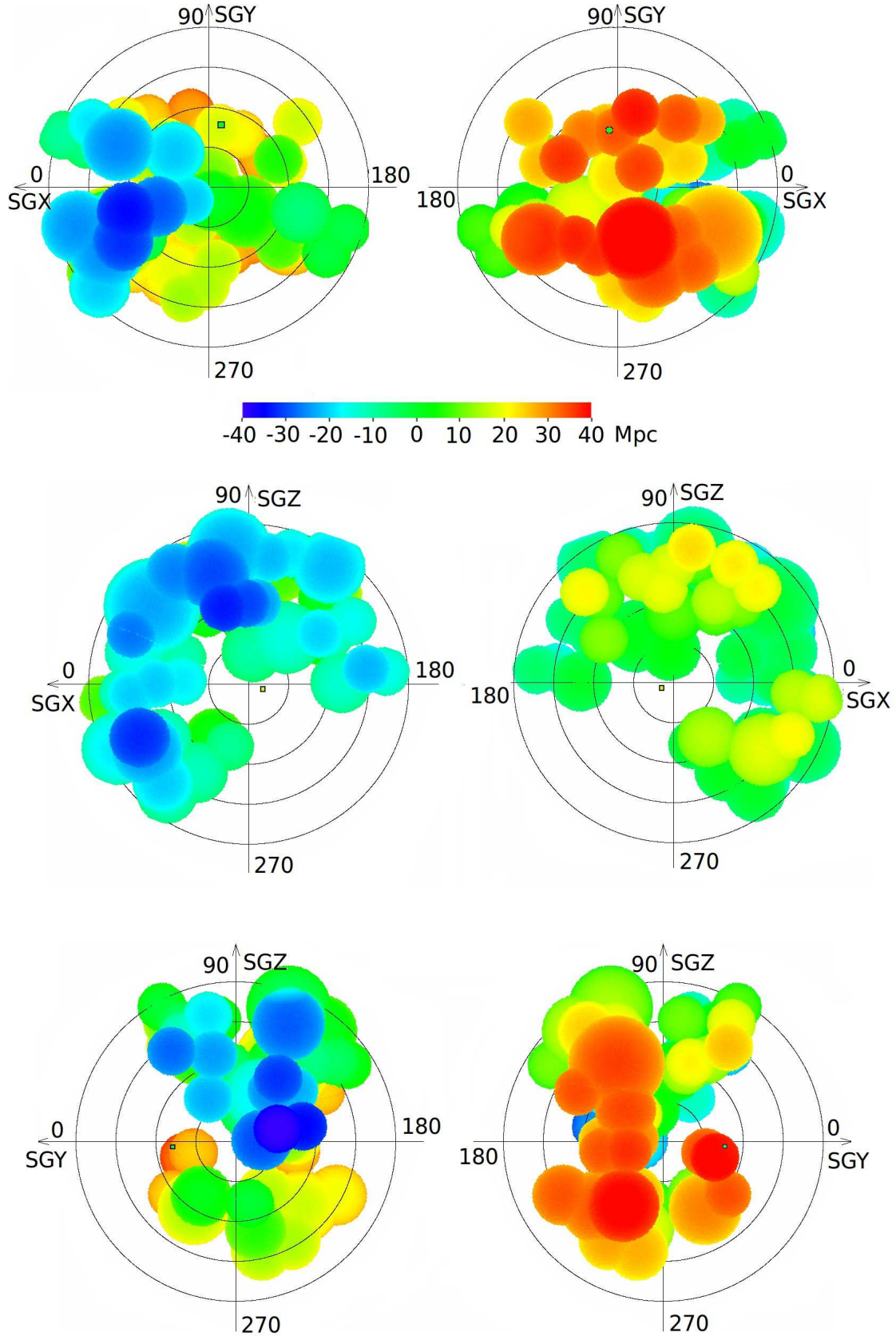


Figure 3: Projection of the HV1 hypervoid on the supergalactic SGX–SGY plane (the top panel), SGX–SGZ (the middle panel), SGY–SGZ (the bottom panel). The view from the negative (left) and positive (right) directions of the Z, Y, X axes is shown in three panels, respectively. The square marks the center of the Virgo cluster. Colors show the distances to the supergalactic plane.

that the galaxy is on the far edge of the considered volume ($D > 40$ Mpc), where different edge effects become significant; (12) notes: the crosses (\times) mark the galaxies from the Catalog of Nearby Isolated Galaxies LOG [25], the pluses ($+$) mark the galaxies from the list of isolated dwarf galaxies in the Local supercluster [26]. The analysis of the data presented in Table 3 allows us to make the following conclusions.

a) The distribution of galaxies in the voids based on morphological types is distinctly shifted towards the latest types: Im, BCD, Ir, as compared to the samples of dwarfs in groups and general field. The dwarf galaxies of the Im, BCD, and Ir types make up about 65%, and along with Sm—up to 85% of the Table 3 sample. Note that among the very isolated galaxies of the LOG catalog [25] the irregular, BCD, and Sm objects represent about 51%. Only in two galaxies, J0817+24 (dEn type) and J1518–24 (Sb? type), their yellowish color indicates the dominance of the old stellar population. Both of them are located near the void surfaces and have neighbors with similar line-of-sight velocity values, i.e. they are members of diffuse groups, adjoining the voids. The excess of irregular blue galaxies and isolated galaxies among the samples of galaxies in the voids was also noted in [30, 31, 32].

b) Among 60 dwarf galaxies in the nearby voids, observed with the GALEX, the FUV-fluxes were not detected in only four of them. Two of these galaxies were mentioned above as the group members and two others are projected on the center of a rich Coma cluster (= Abell 1656). The remaining objects of our sample follow a fairly clear correlation between SFR

Table 3: Dwarf galaxies in the nearby voids

Name	J 2000.0	V_{LG}	Type	B_T	m_{FUV}	$\log F_{HI}$	M_B	$\log M_{HI}$	$\log SFR$	Depth	Notes
(1)	(2)	(3)	(4)	(5)	(6)	(7)	(8)	(9)	(10)	(11)	(12)
ESO149–018	000714.5–523712	1744	Sdm	15.9	17.51	0.74	–16.04	8.87	–1.43	0.5	\times
KK261	004058.7–261605	2726	Ir	17.6	18.20	0.42	–15.31	8.94	–1.32	1.1	
LSBCF682–01	005731.9+102148	2936	SBm	17.9	19.47	0.40	–15.40	8.98	–1.58	–	
ESO541–005	005918.1–203444	2006	Sdm	15.8	17.39	0.91	–16.49	9.16	–1.23	0.4	–
UGC00655	010401.2+415035	1084	Sd	14.4	16.30	1.21	–16.75	8.93	–1.17	0.6	\times
LSBGF352–021	012658.6–350542	2068	BCD	17.5	19.18	0.36	–14.85	8.63	–1.92	4.3	\times
UGC01038	012747.4+431506	1473	Sm	17.0	18.67	0.14	–14.79	8.12	–1.87	0.6	
SDSS	013708.1–003354	3044	Sm	17.1	18.68	0.00	–16.12	< 8.61	–1.36	–	
ESO355–005	021839.7–363152	2399	Sm	17.2	18.45	0.58	–15.46	8.98	–1.50	0.5	\times
ESO298–033	022128.7–384814	2142	Im	16.8	18.53	0.51	–15.62	8.81	–1.64	0.2	+
LCRS	025224.5–411633	3470	BCD	18.1	19.33	< 0.00	–15.37	< 8.72	–1.54	–	
6dF	051556.2–364418	1867	Ir	16.7	18.30	0.14	–15.51	8.33	–1.59	0.3	
ESO306–010	053415.6–391010	1921	Sm	16.7	17.91	0.76	–15.54	8.97	–1.44	2.4	
ESO554–017	053557.2–211451	1385	Sd	16.7	–	< 0.00	–14.83	< 7.93	–	0.6	
UGC03672	070627.6+301919	964	Im	15.4	17.23	1.23	–15.52	8.84	–1.62	1.6	$\times+$
UGC03876	072917.5+275358	811	Scd	13.7	–	1.06	–16.72	8.52	–	0.3	\times
SDSS	080158.9+212219	1343	Ir	17.7	19.69	< 0.00	–13.84	< 7.90	–2.40	6.1	
LCSBS1123P	081715.9+245357	1832	dEn	17.3	>23	0.38	–14.88	8.55	–3.48	0.5	
SDSS	082712.8+265127	1779	Im	17.4	–	–	–14.76	–	–	0.7	\times
SDSS	083641.1+051625	2933	BCD	17.8	18.94	< 0.00	–15.34	< 8.58	–1.50	–	
2MASX	083735.5+074831	1280	BCD	16.7	17.93	0.43	–14.66	8.29	–1.80	1.3	*
CAM0840+1044	084236.6+103314	3437	BCD	17.6	19.21	< 0.00	–15.98	< 8.72	–1.39	–	
SDSS	091001.7+325660	1388	Ir	17.1	18.95	–	–14.39	–	–2.17	1.0	
2MASX	091448.8+330115	1446	BCD	16.8	18.52	–	–14.76	–	–1.97	0.5	
KUG1028+412	103118.4+410226	2568	BCD	17.6	–	–	–15.18	–	–	0.4	\times
SDSS	103950.9+564403	1216	Ir	17.5	17.87	–	–13.64	–	–1.90	–	
HS1059+3934	110209.9+391846	3267	BCD	17.7	18.51	–	–15.63	–	–1.26	–	
APMUKS	110541.0–000602	3160	Sm	18.0	19.47	< 0.00	–15.42	< 8.64	–1.55	–	**
SDSS	112149.2+585434	1596	Ir	17.0	18.65	–	–14.73	–	–1.98	–	
SDSS	124459.3+525203	2808	BCD	18.4	19.45	–	–14.59	–	–1.78	–	
ABELL1656:3237	125941.3+275015	3224	BCD	19.7	>23	–	–13.57	–	–3.10	–	
ABELL1656:2538	130040.1+274851	3495	BCD	20.3	>23	–	–13.14	–	–3.03	–	
SDSS	130905.4+134819	3223	Ir	18.0	20.16	–0.38	–15.32	8.28	–1.92	–	
SDSS	131011.7+135116	3279	BCD	18.1	20.51	–0.25	–15.26	8.42	–2.04	–	
SDSS	133753.5+635510	2813	BCD	17.8	20.52	–	–15.21	–	–2.19	1.0	
SDSS	135031.2–013758	2366	Im	19.0	19.80	< 0.00	–13.80	< 8.39	–1.93	0.8	
KKR2	140626.9+092133	3213	Sm	17.6	19.17	0.26	–15.74	8.92	–1.51	0.6	+
SDSS	151454.6+341439	2910	Im	18.3	19.66	–	–14.79	–	–1.81	–	
2MASX	151844.7–241051	1881	Sb?	16.6	>23	–	–16.13	–	–3.08	0.9	
SDSS	151939.3+385255	3122	BCD	17.5	19.44	–	–15.73	–	–1.68	–	
SDSS	152013.6+400301	2823	BCD	17.8	19.55	–	–15.22	–	–1.80	–	
SDSS	152644.5+403448	2890	BCD	17.8	20.16	–	–15.26	–	–2.03	–	
KKR26	161644.6+160509	2347	Im	17.8	19.03	0.45	–14.93	8.83	–1.67	0.8	$\times+$
LSBCF585–V01	162558.6+203949	2106	Ir	17.9	18.98	0.11	–14.65	8.40	–1.70	4.1	$\times+$
SDSS	163424.7+245741	1131	BCD	18.1	20.40	< 0.00	–13.03	< 7.75	–2.86	0.4	\times
SDSS	170517.4+355222	1184	Im	17.5	18.69	–	–13.65	–	–2.20	0.7	
HIPASS1752–59	175251.4–594049	2596	Ir	17.2	–	0.52	–15.89	8.99	–	0.6	
UGC11109	180414.0+464414	1820	Sm	17.2	18.25	0.72	–14.97	8.88	–1.58	3.9	\times
UGC11220	182325.5+405643	1706	Sm	16.7	17.00	0.98	–15.34	9.08	–1.13	1.7	\times
HIPASS1926–74	192727.1–740458	2444	BCD	17.0	–	0.36	–15.91	8.78	–	2.4	\times
KK246	200357.4–314054	572	Ir	17.1	20.01	0.90	–13.70	8.06	–2.43	4.5	\times ***
6dF	210804.9–471941	832	BCD	15.9	18.12	< 0.00	–14.53	< 7.48	–2.24	0.8	
LSBCF743–01	211845.4+082202	3203	Sm	17.5	18.13	0.46	–16.00	9.11	–0.96	0.6	
CGCG426–040	212006.0+115506	1415	BCD	16.4	18.64	0.34	–15.41	8.28	–1.82	1.7	

Table 3: (Contd.)

Name	J 2000.0	V_{LG}	Type	B_T	m_{FUV}	$\log F_{HI}$	M_B	$\log M_{HI}$	$\log SFR$	Depth	Notes
(1)	(2)	(3)	(4)	(5)	(6)	(7)	(8)	(9)	(10)	(11)	(12)
SDSS	212202.3+095311	3237	BCD	17.7	–	< 0.00	-15.77	< 8.66	–	0.4	
ESO531-001	213152.0-235632	2668	Sm	17.1	18.47	0.09	-15.92	8.59	-1.32	–	
UGC11771	213527.5+232805	1951	Sd	16.4	18.60	0.64	-16.17	8.86	-1.47	0.5	
UGC11813	214731.1+220951	2124	Sm	17.3	19.07	0.71	-15.51	9.01	-1.54	1.5	
SDSS	223036.8-000637	1758	BCD	17.4	–	-0.22	-14.81	7.92	–	0.4	
ADBS	225558.3+261011	2930	BCD	17.7	19.21	0.35	-15.79	8.93	-1.33	0.9	
LSBCF469-02	225721.5+275852	3233	Sm	18.3	18.25	0.46	-15.21	9.12	-1.01	–	×
SDSS	230511.2+140346	1801	BCD	17.3	19.38	< 0.00	-15.52	< 8.15	-1.52	0.3	
6dF	231803.9-485936	2275	BCD	16.9	18.42	< 0.00	-15.62	< 8.36	-1.56	3.8	×
KKR75	232011.2+103723	1703	Ir	18.0	19.48	0.54	-14.05	8.65	-2.11	1.9	×+
LSBCF750-04	234420.2+100705	1726	Sd	17.3	18.62	0.40	-14.80	8.51	-1.74	0.7	
UGC12771	234532.7+171512	1535	Im	16.9	18.35	0.46	-14.96	8.48	-1.72	0.4	×+
APMUKS	234650.9-301106	2926	BCD	18.2	19.61	< 0.00	-14.89	< 8.58	-1.80	0.7	
LSBCF750-V01	235419.6+105636	1164	Ir	18.0	19.66	< 0.00	-13.41	< 7.78	-2.37	0.4	

Notes:

* The LEDA specifies a significant difference in the heliocentric velocity estimates of this galaxy from the SDSS optical data ($+1452 \pm 19$ km/s) and from the HI measurements in the HIPASS ($+2006 \pm 8$ km/s). Re-processing of the optical spectrum yields $+2004 \pm 15$ km/s, which is close to the HIPASS estimate.

** The line-of-sight velocity value of this the galaxy, obtained in [45] needs to be confirmed.

*** Column (3) indicates the formal value of the line-of-sight velocity, corresponding to the distance of the galaxy 7.83 Mpc [9] and the parameter $H_0 = 73$ km/s/Mpc. Having the line-of-sight velocity of $V_{LG} = +436$ km/s, this galaxy is moving to us from the depth of the void with the peculiar velocity of -130 km/s.

and absolute magnitude of the galaxy (see Fig. 4) with the $R = -0.82$ correlation coefficient and the median value of the specific star formation rate $SSFR = 1 \times 10^{-10} M_{\odot} \text{ yr}^{-1} L_{\odot}^{-1}$, typical of the late-type dwarfs in the Local Volume [33].

c) The distribution of dwarf galaxies in the voids based on the hydrogen mass logarithm and B -luminosity is shown in Fig. 5 by the solid circles. The upper limits of the hydrogen mass estimates M_{HI} are shown by unfilled circles. As follows from these data, the dwarfs in the voids have a high hydrogen abundance per luminosity unit. The median value for them, $M_{HI}/L_B = 2.1 M_{\odot}/L_{\odot}$ proves to be approximately three times higher than for the Ir, Im, and BCD galaxies in the groups and general field [34]. In other words, dwarf galaxies in the voids possess increased gas reserves compared to the galaxies of the same type located in denser environments, what was repeatedly mentioned by different authors [17, 26, 35, 36, 37, 43, 44]. Possessing normal star formation rates (SFR) per luminosity unit, $\log SSFR \simeq -10$, the dwarfs in the voids are able to maintain the observed SFR on the scale of about 20–30 Gyr. At the same time, the studies [31, 38] considering the properties of galaxies in the voids in much larger volumes ($z < 0.09$) demonstrate that although in general the void galaxies are bluer and fainter than the cluster galaxies, however, in the same luminosity range no differences in colors or SFRs are observed.

d) Figure 6 shows the distribution of 48 galaxies in the nearby ($D < 40$ Mpc) voids by the absolute magnitude and the depth of bedding under the hypervoid’s surface. We can see that only a quarter of these galaxies are located in the voids at depths exceeding 1.5 Mpc. Recall that in our algorithm the accuracy with which the position of the spherical void center was determined was exactly 1.5 Mpc. Consequently, plenty of dwarf galaxies in this boundary layer can be located outside the voids. In any case, the population of dwarf galaxies in the cores of voids (Depth > 1.5 Mpc) is represented literally by single objects, such as their nearest and most famous representative KK 246 [39, 40, 41]. Note that only 4 out of 13 galaxies that are located in the middle of voids are “new”. The nine remaining objects are specified as isolated in the lists of [25, 26]. Since the selection criteria in this and the two above studies were completely different, we have to expect that these nine galaxies are very isolated objects. In Fig. 6 and Table 3 all the galaxies, identified with the objects from the lists of [25, 26] are marked by the corresponding signs.

Despite the poor statistics, note a certain tendency of declining dwarf galaxy luminosity with increasing depth below the hypervoid surface. The same feature was noted earlier by Chengalur and Pustilnik [42]. From general considerations we may assume that such objects have record low metallicities. This makes them interesting for the spectral observations.

e) All the dwarf galaxies we have discovered in the nearby voids have absolute magnitudes brighter than -13^m . Their distribution by distance and absolute magnitude in Fig. 7 shows that this limit may be due to the distance selection effect. However, the nature of the data in Fig. 7 does not contradict the assumption about the existence of a luminosity threshold, $M_B \simeq -13.0^m$ in the dwarf population of voids. This circumstance may have a vital importance for understanding the nature of empty cosmic volumes.

6 CONCLUDING REMARKS

To search for empty volumes in the Local Universe, we used an algorithm similar to the approach of Patiri et al. [14], only with a much more stringent restriction on the luminosity of galaxies, evading the voids. As a result we have obtained a list of nearby spherical voids with the typical diameter of 15 Mpc, which is about three times smaller than that in [14]. However, the total volume of our voids is about 30% of the volume of the Local Universe within 40 Mpc. The distribution of the centers of spherical voids proved to be very far from the Poisson distribution. More than 90% of the voids overlap, forming three hypervoids composed of 56, 22 and 5 initial voids, respectively. The closest and most populated hypervoid HV1 comprises the Tully Local Void and extends in a horseshoe shape, covering the central region of the Local Supercluster of galaxies.

Eighty-nine voids we have identified with the center distances within < 40 Mpc from us contain 48 late-type dwarf galaxies with absolute magnitudes in the range of $M_B = [-13.0, -16.7]$. These galaxies have active star formations and gas reserves per luminosity unit by about 2–3 times higher than those in the dwarf galaxies of the same type, located in denser environments. The abundance of neutral hydrogen in void galaxies was repeatedly noted by different authors [17, 26, 35, 36, 37, 43, 44]. The void dwarfs reveal a tendency of evading the depths of the voids and hypervoids. In fact, the central regions of voids are devoid of not only normal, but also dwarf galaxies. According to a rough estimate, in the hearts of the voids having the sizes of about a half of the diameter, the average stellar mass density is two orders lower than the average cosmological density.

We should note here the following important fact. We have defined the contours of the nearby voids and identified the dwarf population there in the space of radial velocities rather than that of actual distances. The presence of collective motions of galaxies with the amplitudes of 300 km/s can lead to a significant distortion of void shapes and the global pattern of their distribution. Obviously, this situation will gradually become clearer as more and more data is obtained on the individual distances of galaxies.

As we can see from Table 3, about one-third of dwarf galaxies in the nearby voids ensue from the photometric and spectral sky survey SDSS [13]. An extension of this fruitful survey to the other remaining regions of the northern sky, as well as a prospective similar mass survey in the southern sky will soon allow us to better understand the characteristics of the dwarf population of voids, in particular, to find out whether there exist any ultra-faint dwarf objects with luminosities fainter than $3 \times 10^7 L_\odot$ and hydrogen masses lower than $10^7 M_\odot$ in the empty cosmic volumes.

Acknowledgments

The present study has made use of the SDSS (<http://www.sdss.org>), HyperLeda (<http://leda.univ-lyon1.fr>) and NED (<http://nedwww.ipac.caltech.edu>) databases. This study was made owing to the support of the following grants: the grants of the Russian Foundation for Basic Research (project nos. 12-02-91338-NNIO, 11-02-00639, 11-02-90449-Ukr-f-f, the State Foundation for Basic Research of the Ukraine F40.2/49, the Cosmomicrophysics program of the National Academy of Sciences of the Ukraine, as well as by the Ministry Education and Science of the Russian Federation (state contract no. 14.740.11.0901) and project 2012-1.5-12-000-1011-004.

References

- [1] M. Joeveer, J. Einasto, and E. Tago, *MNRAS*, **185**, 357 (1978).
- [2] S. A. Gregory and L. A. Thompson, *ApJ*, **222**, 784 (1978).
- [3] R. P. Kirshner, A. Oemler, P. L. Schechter, and S. A. Shectman, *ApJ*, **248**, L57 (1981).
- [4] U. Lindner, J. Einasto, M. Einasto, et al., *A&A*, **301**, 329 (1995).
- [5] A. V. Tikhonov and I. D. Karachentsev, *ApJ*, **653**, 969 (2006).
- [6] R. van de Weygaert and E. Platen, arXiv:0912.2997 (2009).
- [7] P. J. E. Peebles, *ApJ*, **557**, 495 (2001).
- [8] R. B. Tully and J. R. Fisher, *Nearby Galaxies Atlas*, (Cambridge Univ. Press, Cambridge, 1987).
- [9] I. D. Karachentsev, A. E. Dolphin, R. B. Tully, et al., *AJ*, **131**, 1361 (2006).
- [10] T. P. McIntyre, R. F. Mibchin, E. Momjian, et al., *ApJ*, **739**, 26 (2011).
- [11] O. G. Nasonova and I. D. Karachentsev, *Astrophysics*, **54**, 1 (2011).
- [12] M. Colless, G. Dalton, S. Maddox, et al., *MNRAS*, **328**, 1039 (2001).
- [13] K. N. Abazajian, J. K. Adelman-McCarthy, M. A. Aqueros, et al., *ApJ Supplement*, **182**, 543 (2009).
- [14] S. G. Patiri, J. Betancort-Rijo, F. Prada, et al., *MNRAS*, **369**, 335 (2006).
- [15] F. Hoyle, M. S. Vogeley, and D. Pan, arXiv:1205.1843 (2012).
- [16] A. Fairall, *Large-Scale Structures in the Universe* (Wiley, New York, 1998).
- [17] S. A. Pustilnik and A. L. Tepliakova, *MNRAS*, **415**, 1188 (2011).
- [18] A. Saintonge, R. Giovanelli, M. P. Haynes, et al., *AJ*, **135**, 588 (2008).
- [19] R. Giovanelli, M. P. Haynes, B. R. Kent, et al., *AJ*, **130**, 2598 (2005).
- [20] I. D. Karachentsev, V. E. Karachentseva, O. V. Melnyk, et al., *Astrophysical Bulletin*, **67**, 353 (2012).

- [21] G. Paturel, C. Petit, P. Prugniel, et al., *A&A*, **412**, 45 (2003).
- [22] T. N. Jarrett, T. Chester, R. Cutri, et al., *AJ*, **119**, 2498 (2000).
- [23] S. Tavasoli, K. Vasei, and R. Mohayaee, arXiv:1210.2432; submitted to MNRAS.
- [24] H. M. Courtois, Y. Hoffman, R. B. Tully, and S. Gottloeber, *ApJ*, **744**, 43 (2012).
- [25] I. D. Karachentsev, D. I. Makarov, V. E. Karachentseva, and O. V. Melnyk, *Astrophysical Bulletin*, **66**, 1 (2011).
- [26] V. E. Karachentseva, I. D. Karachentsev, and M. E. Sharina, *Astrophysics* **53**, 462 (2010).
- [27] D. C. Martin, J. Fanson, D. Schiminovich, et al., *ApJ*, **619**, L1 (2005).
- [28] Gil de Paz A., S. Boissier, B. F. Madore, et al., *ApJ Supplement*, **173**, 185 (2007).
- [29] J. C. Lee, A. Gil de Paz, R. C. Kennicutt, et al., *ApJ Supplement*, **192**, 6 (2011).
- [30] F. Hoyle, R. R. Randall, M. S. Vogeley, and J. Brinkmann, *ApJ Supplement*, **620**, 618 (2005).
- [31] S. G. Patiri, F. Prada, J. Holtzman, et al., *ApJ Supplement*, **372**, 1710 (2006).
- [32] I. B. Vavilova, O. V. Melnyk, and A. A. Elyiv, *Astron. Nachr.* **330**, 1004 (2009).
- [33] I. D. Karachentsev, D. I. Makarov, and E. I. Kaisina, submitted to *ApJ Supplement*.
- [34] I. D. Karachentsev, V. E. Karachentseva, W. K. Huchtmeier, and D. I. Makarov, *AJ*, **127**, 2031 (2004).
- [35] W. K. Huchtmeier, U. Hopp, and B. Kuhn, *A&A* **319**, 67 (1997).
- [36] S. A. Pustilnik, J. M. Martin, W. K. Huchtmeier, et al., *A&A* **389**, 405, (2002).
- [37] S. A. Pustilnik, J. M. Martin, A. L. Tepliakova, and A. Y. Kniazev, *MNRAS*, **417**, 1335 (2011).
- [38] G. Sorrentino, V. Antonuccio-Delogu, and A. Rifatto, *A&A* **460**, 673 (2006).
- [39] A. Begum, J. N. Chengalur, I.D. Karachentsev, et al., *MNRAS*, **386**, 1667 (2008).
- [40] K. Kreckel, P. J. E. Peebles, J. H. van Gorkom, et al., *AJ*, **141**, 204 (2011).
- [41] G. Gentile, G. V. Angus, and B. Famaey et al., *A&A*, **543**, A47 (2012).
- [42] J. N. Chengalur and S. A. Pustilnik, *MNRAS*, (in press).
- [43] R. Stanonik, E. Platen, M. A. Aragon-Calvo, et al., *Astronom. Soc. Pacific Conf.* **421**, 107 (2010).
- [44] K. Kreckel, E. Platen, M. A. Aragon-Calvo, et al., *AJ*, **144**, 16 (2012).
- [45] C. Impey, V. Burkholder, and D. Sprayberry, *AJ*, **131**, 2341 (2001).

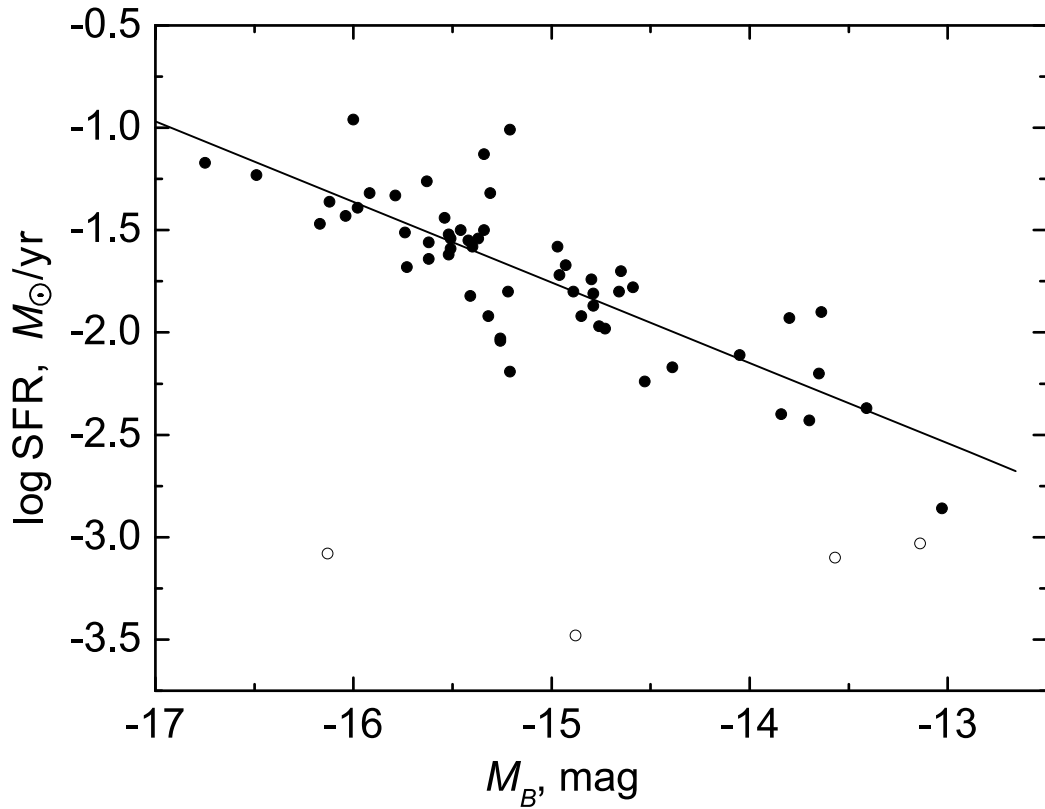


Figure 4: Relationship between the logarithm of star formation rate SFR and absolute magnitude M_B for 60 dwarf galaxies in the voids. The unfilled circles show the galaxies with upper estimates of m_{FUV} , which were not accounted for in the regression parameters: $\log \text{SFR} = -0.39M_B - 7.65$, $R = -0.82$, $\text{SD} = 0.22$, where R is the correlation coefficient, and SD is the RMS deviation.

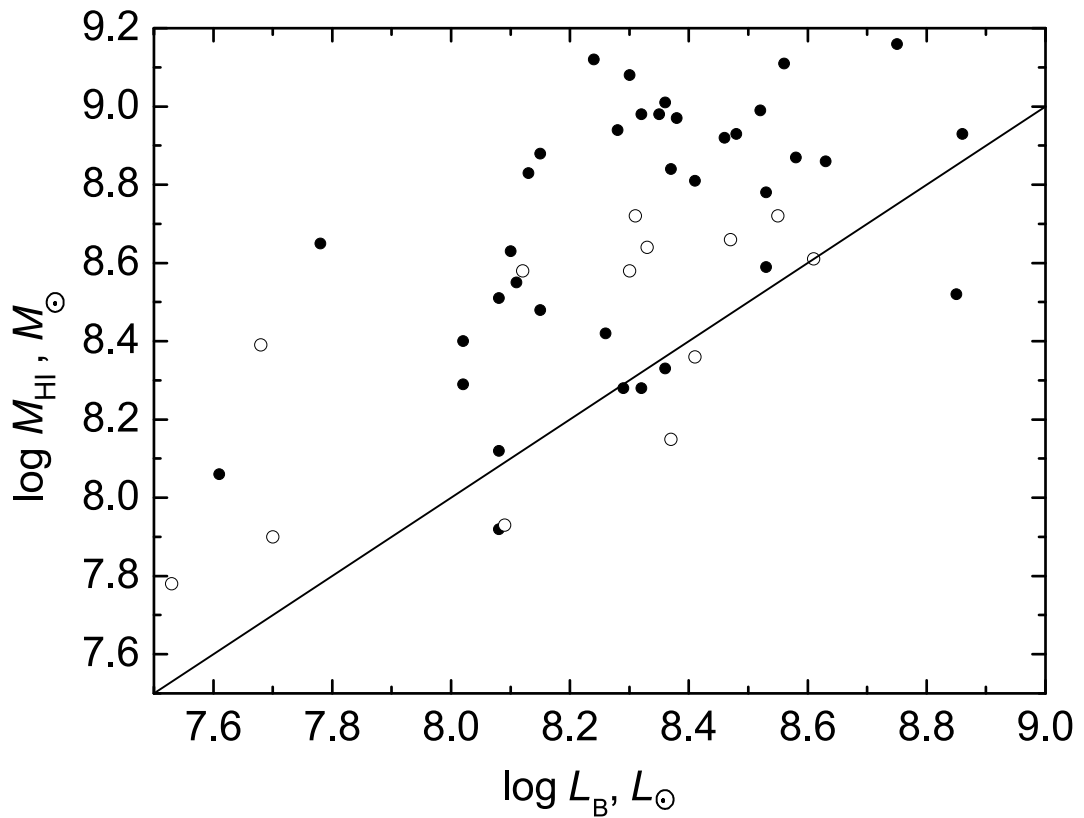


Figure 5: Distribution of 51 dwarf galaxies in the voids by hydrogen mass logarithm and B -luminosity. Open symbols mark the objects with an upper limit estimate of M_{HI} . The straight line corresponds to $M_{\text{HI}}/L_{\text{B}} = 1 M_{\odot}/L_{\odot}$.

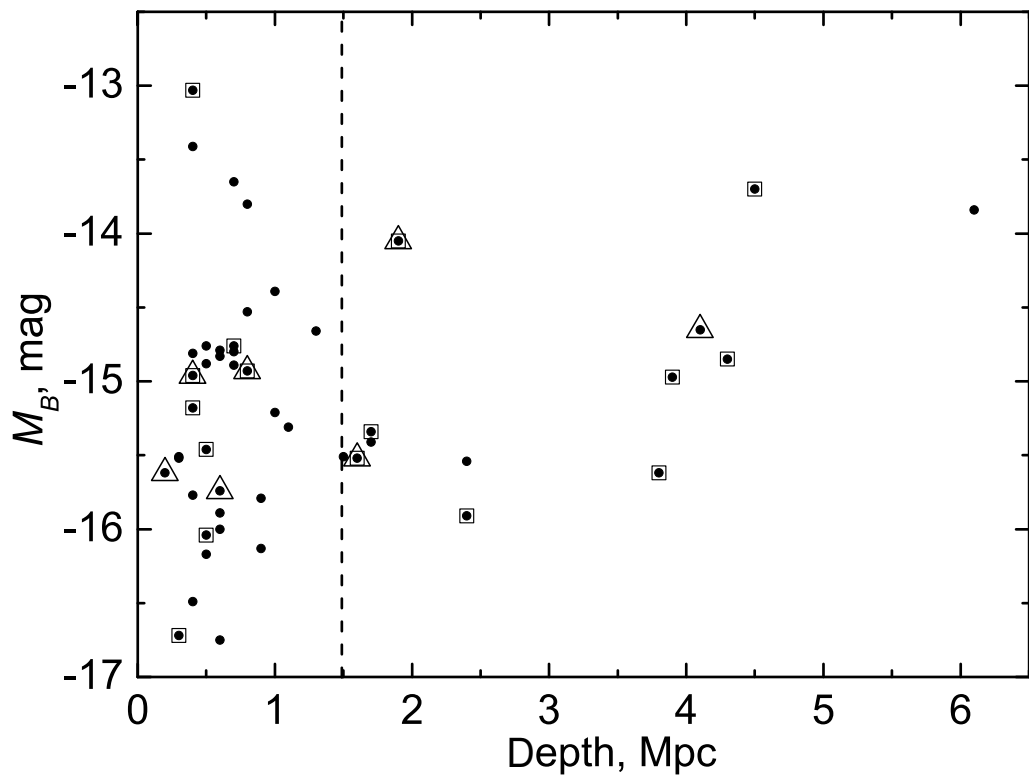


Figure 6: Distribution of 48 dwarf galaxies in the nearby ($D < 40$ Mpc) voids by absolute magnitude M_B and the bedding depth under the surface of hypervoid. Squares trace the objects common with the galaxies from the Catalog of Nearby Isolated Galaxies [25], triangles denote the late-type dwarf galaxies from the list of [26].

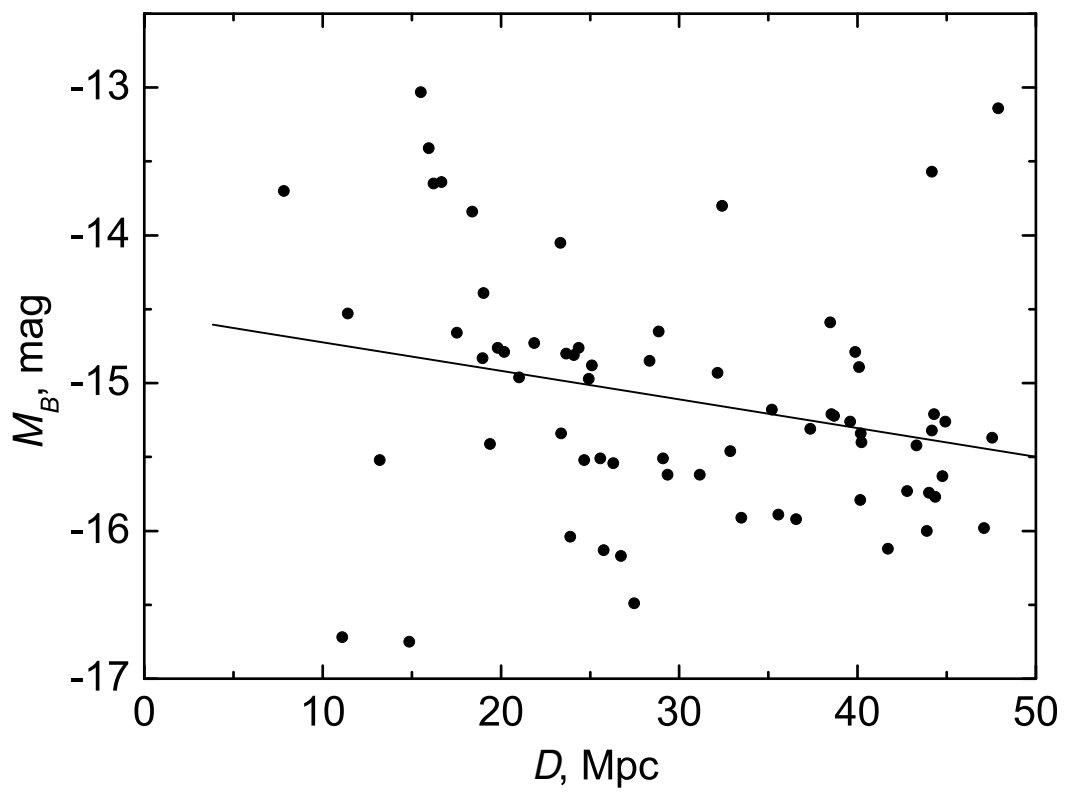


Figure 7: Distribution of 68 dwarf galaxies by absolute magnitude M_B and distance from the observer. The regression parameters are as follows: $M_B = -0.02D - 14.53$, $R = -0.26$, $SD = 0.8$.